

Geology and C-O isotope geochemistry of carbonate-hosted Pb-Zn deposits, NW Guizhou Province, SW China

DOU Song^{1,3} and ZHOU Jiayi^{2*}

¹ Yunnan Nonferrous Metals Geological Bureau, Kunming 650051, China

² State Key Laboratory of Ore Deposit Geochemistry, Institute of Geochemistry, Chinese Academy of Sciences, Guiyang 550002, China

³ School of Geoscience and Info-Physics, Central South University, Changsha 410083, China

* Corresponding author, E-mail: zhoujiayi@vip.gyig.ac.cn

Received November 11, 2011; accepted April 22, 2012

© Science Press and Institute of Geochemistry, CAS and Springer-Verlag Berlin Heidelberg 2013

Abstract The Pb-Zn metallogenic district in NW Guizhou Province is an important part of the Yunnan-Sichuan-Guizhou Pb-Zn metallogenic province, and also is one of the most important Pb-Zn producers in China. The hosting rocks of the Pb-Zn deposits are Devonian to Permian carbonate rocks, and the basement rocks are meta-sedimentary and igneous rocks of the Proterozoic Kunyang and Huili groups. The ore minerals are composed of sphalerite, galena and pyrite, and the gangue minerals are include calcite and dolomite. Geology and C-O isotope of these deposits were studied in this paper. The results show that $\delta^{13}\text{C}$ and $\delta^{18}\text{O}$ values of hydrothermal calcite, altered wall rocks-dolostone, sedimentary calcite and hosting carbonate rocks range from -5.3‰ to -0.6‰ (mean -3.4‰) and +11.3‰ to +20.9‰ (mean +17.2‰), -3.0‰ to +0.9‰ (mean -1.3‰) and +17.0‰ to +20.8‰ (mean +19.7‰), +0.6‰ to +2.5‰ (mean +1.4‰) and +23.4‰ to +26.5‰ (mean +24.6‰), and -1.8‰ to +3.9‰ (mean +0.7‰) and +21.0‰ to +26.8‰ (mean +22.9‰), respectively, implying that CO_2 in the ore-forming fluids was mainly a result of dissolution of Devonian and Carboniferous carbonate rocks. However, it is difficult to evaluate the contribution of sediment de-hydroxylation. Based on the integrated analysis of geology, C and O isotopes, it is believed that the ore-forming fluids of these carbonate-hosted Pb-Zn deposits in this area were derived from multiple sources, including hosting carbonate rocks, Devonian to Permian sedimentary rocks and basement rocks (the Kunyang and Huili groups). Therefore, the fluids mixing is the main precipitation mechanism of the Pb-Zn deposit in this province.

Key words C and O isotopes; source of ore-forming fluids; NW Guizhou Pb-Zn metallogenic province; SW China

1 Introduction

Located in the western margin of the Yangtze block, the carbonate-hosted Pb-Zn metallogenic district in NW Guizhou Province is one of the most important Pb-Zn producers in China and also an important part of the Chuan (Sichuan)-Dian (Yunnan)-Qian (Guizhou) carbonate-hosted Pb-Zn metallogenic province (CDQ province) (Fig. 1). Pb-Zn ores in this province have been prospected and mined for several decades. The accumulated Pb+Zn metals reserves more than 5 million tons (Jin Zhongguo, 2008). There are more than 100 Pb-Zn deposits in this province, 9

of which are medium-sized (Pb+Zn metals reserves more than 0.2 Mt) deposits and 40 are small-sized ones (Pb+Zn metals reserves less than 0.2 Mt) (Fig. 2).

The geology study of these deposits can be traced back to the 1960s (Xie Jiarong, 1963), whereas geochemical research on the deposits started from 1980s. Great achievement on geology, structure, and magmatic activities are gained with different opinions about the sources of ore-forming fluids. For example, Chen Shijie (1984, 1986) and Tang Shengning (1984) proposed that the ore-forming fluids were derived from the hosting rocks. On the other hand, Zheng

Chuanlun (1992, 1994) suggested that the ore-forming fluids were sourced from Devonian to Permian sedimentary rocks and basement rocks (Mao Deming, 2000, 2001; Qian Jianping, 2001). There are also models that favor involvement of multiple sources, including the hosting rocks, Devonian to Permian sedimentary rocks, basement rocks and Permian flood basalts for the ore-forming fluids (e.g. Liu Hechang, 1996; Hu Yaoguo, 1999; Liu Hechang and Lin Wenda, 1999; Han Runsheng et al., 2001; Huang Zhilong et

al., 2004). However, Gu Shangyi (2006, 2007) believed that there is no genetic relationship between Permian flood basalts and the formation of the deposits in the province, but just a coincidence in space distribution between basalts and deposits.

In this paper, we present systematic analyses of carbon and oxygen isotope and geology in detail, together with previously published data to discuss the possible ore-forming fluids sources of the deposits.

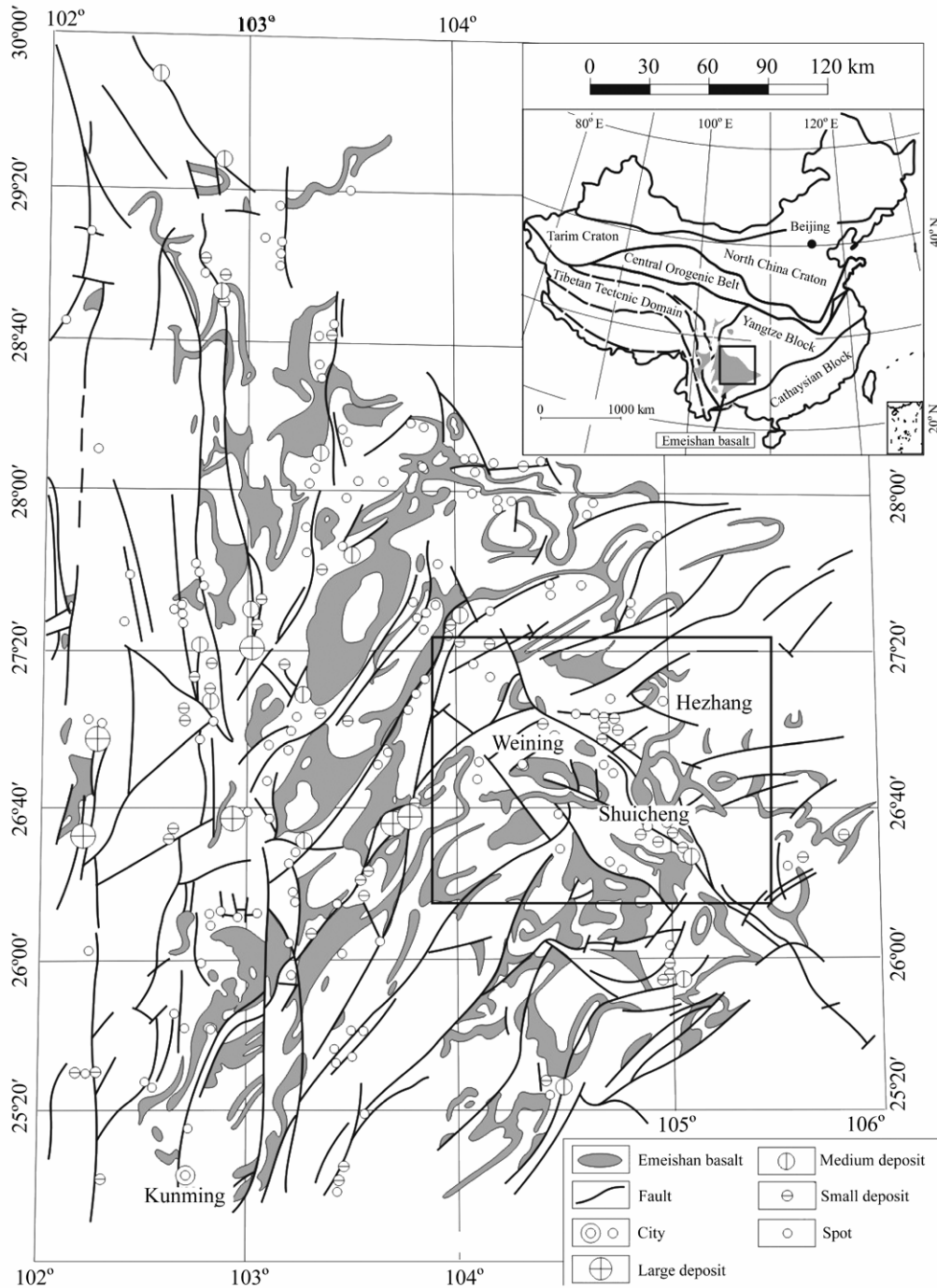


Fig. 1. Regional geological sketch map of the CDQ Pb-Zn metallogenic province.

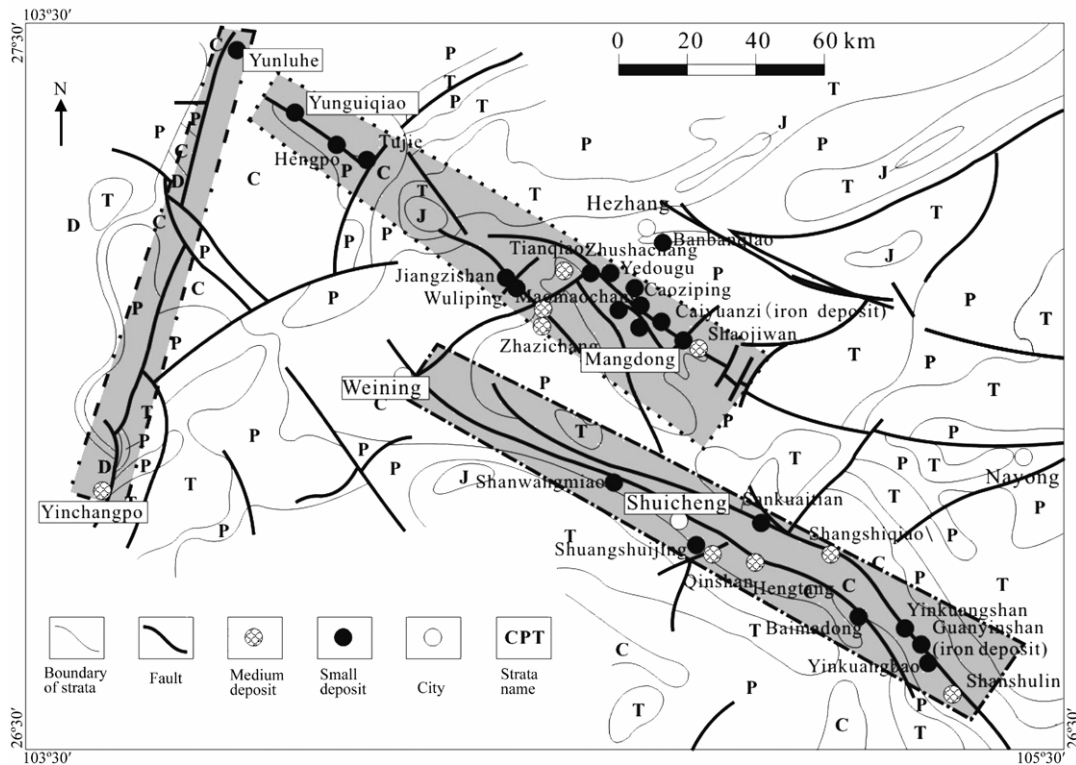


Fig. 2. Regional geological sketch map of the NW Guizhou Pb-Zn metallogenic district.

2 Geological background

2.1 Regional geology

Located in the western Yangtze block, the carbonate-hosted Pb-Zn metallogenic province in NW Guizhou Province is controlled by the Yinchangpo-Yunluhe, Weining-Shuicheng and Yunguiqiao-Mangdong faults (Fig. 2). The basement rocks of the Yangtze block include Proterozoic Dongchuan, Kunyang and Huili groups in the northern part and widespread Neoproterozoic sedimentary sequences in the southeastern part (Wang Wei and Zhou Meifu, 2012). Lithologically, the Kunyang and Huili groups are mainly composed of mid-depth metamorphic complex rocks, metamorphic fine-clastic rocks, metamorphic volcanic-sedimentary rocks, shallow metamorphic fine-clastic rocks and carbonate rocks.

The sedimentary cover is mainly Devonian, Carboniferous and Permian in ages, and the widespread distributed Emeishan flood basalts (Jin Zhongguo, 2008). Lithologically, the sedimentary rocks are mainly composed of carbonate rocks, shale and sandstone. The Devonian to Permian carbonate rocks are important hosting rocks of the Pb-Zn deposits. Detailed information about the strata is presented in the stratigraphic column (Fig. 3).

2.2 Regional tectonic features

On a regional scale, NW and NNE structural systems mainly grow and they are characterized by thrust faults and tight folds. Based on the faults distribution, the faults in the province can be divided into three groups (Jin Zhongguo, 2008; Zhou Jiayi et al., 2010a, b): (1) The Yunguiqiao-Mangdong fault belt: a fault incised into the basement rocks and composed of a series of high dip-angle reversed faults, which extend along the direction of NW 310° and have a dip angle ranging from 70° to 85°. It extends into Yunnan Province along the NW direction and has a length up to 350 km in Guizhou Province. (2) The Weining-Shuicheng fault belt: consisting of the NW Wei-Shui anticline, Shuishan anticline and longitudinal faults such as the Shuicheng fault accompanied with the Shuishan anticline. This belt undergone intensive compression deformation, which can be evidence by expression in growth of a large amount of cleavages between strata, striations on fault planes, cleavage plane formed by pressure solution and structural lens-shaped bodies in the wing of the fold belt. All of the fold belt's longitudinal faults are high-angle reverse faults and the planes are inclined along the SW or NE direction and have a dip angle ranging from 70° to 80°. Transverse and oblique faults in the fold belt are more mature. (3) The Yinchangpo-Yunluhe

Erathem	System	Series	Formation	Lithology	Thickness (m)	Lithological character
Palaeozoic	Permian	Middle	Longtan (P _{2l})		147-360	Gray-yellow sandstone, shale and claystone, the main coal host strata, pseudoconformity with the below strata
			Emeishan basalt (P _{2β})		>400	Grey-brown massive, amygdaloidal and vesiculate basalt, in middle-above occurs purple vein or lenticular altered basalt and accidentally see lamellar copper, discordant contact the below strata
		Lower	Qixia-Maokou (P _{1q+m})		>400	Dark-grey, grey and light-grey limestone, dolomitic limestone, the dolomitic matter occur as tiger-spot in limestone, conformable contact with the below strata
			Liangshan (P _{1l})		80-187	Gray-deep gray, line-heavy bedded quartz sandstone, thin layered calcareous shales and coal. The lower is argillaceous siltstone, contain nodular hematite
	Carboniferous	Upper	Maping (C _{2m})		189-347	Purple and grey-purple syngenetic pebble limestone, dolomitic limestone, bioclastic limestone, the middle mix up yellow-green shale and limestone (ore-bearing)
			Huanglong (C _{2h})		137-647	Light grey limestone mix up oolitic limestone, the bottom is dolomitic limestone, conformable contact with the below strata, dolomitic banded limestone and bioclastic limestone. The one main Pb-Zn ore-bodies host stratum of this region
		Lower	Baizuo (C _{1b})		183-296	Upper: light gray-grey limestone and grey coarse dolomite, dolomitic banded limestone and bioclastic limestone. The main Pb-Zn ore-bodies host stratum in this region Lower: gray-deep gray, medium-heavy bedded limestone, phycophyta fossil bearing
			Datang (C _{1d})		110-143	Upper: gray-grey medium-coarse limestone, intercalated with grayish yellow, thin layered calcareous shale and dolomitic limestone (subordinate ore-bearing bed) Lower: black layered calcareous shales and limestone of micrite muscovite quality. Pb-Zn ore-bodies hosted in dolomite and parts of limestone
	Devonian	Upper	Rongxian (D _{3r})		119-647	Upper: gray-heavy bedded medium-coarse dolomite (subordinate ore-bearing bed). Pb-Zn ore bodies hosted in light colored coarse crystalline dolomite Middle: grey, medium to thick layered, siliceous dolomite intercalated with grayish yellow, thin layered calcareous shale Lower: light gray-grey, medium-heavy bedded limestone, banded limestone, micritic calcite dolomite, and dolomitic limestone
		Middle	Dushan (D _{2d})		110-380	Gray-white heavy bedded fine-coarse grain dolomite, intercalary with banded limestone. Stromatopora fossil-bearing fine dolomite Black-gray siltstone, intercalary with gray quartz sandstone and oolitic hematite lens

Fig. 3. Stratigraphic column of the NW Guizhou Pb-Zn metallogenic province.

fault belt is located in the east of the Zhaotong-Qujing buried deep fault belt (Han Runsheng et al., 2007). This belt is the NE extension of the Kuangshanchang and Qilingchang tectonic belts in the Huize Pb-Zn deposit (Han Runsheng et al., 2007), and also an important NE mineralizing belt in NW Guizhou Province (Fig. 2).

2.3 Regional magmatic activity

The magmatic activity in the Pb-Zn metallogenic province is intensive with abundant eruptive and intrusive rocks (Fig. 1). The Permian flood basalts in the region are part of the Emeishan large igneous province produced by a mantle plume (Zhou Meifu et al., 2002).

3 Geology of metallogenic belts

3.1 General description

Hosted in 14 ore-bearing rock units, there are over 100 ore deposits in the Pb-Zn metallogenic district in the NW Guizhou Province. The hosting rocks are Devonian to Permian carbonate rocks. The ore bodies are mainly hosted in the Devonian to Carboniferous dolomites and dolomitic limestone. Ore bodies are obviously controlled by the faults, basically along the regional tectonic belt and are outcropped in a linear distribution. In accordance with its fault distribution, the province is divided into three metallogenic belts, named the Weining-Shuicheng (south metallogenic belt), the Yuguizhao-Mangdong (north metallogenic belt) and the Yinchangpo-Yunluhe (west metallogenic belt) metallogenic belts (Fig. 2).

Within the south metallogenic belt, there is Carboniferous to Permian strata. Lithologically, these strata are composed of limestone, dolomite, dolomitic limestone and marl, with minor sandy shale. Most hosting rocks in this belt are limestone of the Upper Carboniferous Huanglong Formation and Maping Formation, and the rest are dolomites of the Lower Carboniferous Datang Formation and Baizuo Formation. Main ore deposits in this belt include the Qingshan and Shanshulin medium Pb-Zn deposits (Pb+Zn metals reserves more than 0.2 Mt), Shangshiban, Shuanglongjing and Hengtang small Pb-Zn deposits (Pb+Zn metals reserves less than 0.2 Mt).

In the north metallogenic belt, there are Devonian, Carboniferous and Permian strata. The Devonian strata are distributed in the central part of the Yuguizhao-Mangdong fault. Ore-bearing rocks mainly include carbonate rocks of the Upper Devonian Rongxian Formation, Lower Carboniferous Datang Formation, Upper Carboniferous Huanglong and

Maping formations, and Lower Permian Qixia-Maokou Formation. This belt has the main lithological characters of coarse-grained dolomite, dolomitic limestone, and limestone, with minor purple red sandstone, shale and marl. Ore bodies are distributed in intersections between multiple faults in a concentrated manner, such as the Caiyuanzi large siderite deposit, Tiekuangshan medium siderite deposit, Yadu, Mangdong, Shaojiwan, Tianqiao, Maomaochang-Zhazichang, Wuliping, Yunguiqiao, Caoziping, Yangjiaochang and Baimachang Pb-Zn deposits, of which the Shaojiwan, Maomaochang-Zhazichang and Tianqiao Pb-Zn deposits are medium ones. They are mainly vein and lens-shaped, which are likely formed in the tectonic crushed zones of the regional faults and its sub inter-laminar compressional fault.

In the western metallogenic belt, there are Carboniferous, Devonian and Permian strata. Ore-bearing rocks include carbonate rocks of the Lower Carboniferous Formation and Upper Carboniferous Huanglong Formation. Most hosting rocks are coarse-grained dolomite and dolomitic limestone. NE-trending faults and Pb-Zn deposits are distributed with the tectonic grows or compounds, while most ore bodies are outcropped in the Yinchangpo-Yunluhe fault belt and its intersections with multiple faults. Ore deposits include the Yinchangpo medium Ag-Pb-Zn and Yunluhe small Pb-Zn deposits.

3.2 Ore types, structures and textures, and wall rocks alteration

The main ore types are oxide ores in the upper parts of each deposit, with mixed ores containing both oxide and sulfide ores in the middle parts, and sulfide ores in the deeper parts. The ores include massive ores (including sphalerite ore, sphalerite-galena ore and galena-pyrite ore) and disseminated ores (including sphalerite ore, sphalerite-galena ore and galena-pyrite ore). The principal ore textures are subhedral, euhedral granular, metasomatic-resorption, and fracture-infill textures, as well as graphic, skeletal, and exsolution textures (Fig. 4). Euhedral-subhedral-anhedral granular textures and microcrystalline to coarse-crystalline granular textures are mostly common. Ore structures are dominated by massive accumulations of sulfide minerals, whereas veined, disseminated and brecciated structures are also presented. The wall-rock has experienced major alterations including dolomitization, pyritization, Fe-Mn carbonation, ferritization, calcitization and silicification.

3.3 Ore mineralogy

Dominant ore minerals in the NW Guizhou

Pb-Zn metallogenic province are galena, sphalerite, and pyrite, with minor chalcopyrite, smithsonite, matildite, acanthite, freibergite, and chlorarargyrite. Gangue minerals are calcite and dolomite, with minor barite, gypsum, quartz, and clay minerals. Sphalerite is fine- to macro-crystalline, anhedral to euhedral, and granular (0.05–30 mm). There are three main stages of sphalerite with distinct color, early stage sphalerite is brown to dark brown; the second stage is reddish brown, yellowish brown; and the late stage sphalerite is light yellow. Sphalerite is present as massive, banded, and disseminated aggregates, coexisting with galena, pyrite, and calcite. The mineral textures present skeletal crystals of pyrite, exhibit estuary, relics, and containment. Large, coarse-grained (0.25–6 mm) sphalerite crystals are common within corrosion cavities (Fig. 4d). In addition, zoned growing textures also present.

Galena occurs as fine- to coarse-grained, anhedral granular aggregates, 0.2–35 mm in size. Stress deformation is obvious, and exsolution textures are common. Galena generally coexists with sphalerite, pyrite, and calcite (Fig. 4h).

Pyrite occurs in four stages. Anhedral to subhedral, granular and sometimes colloform pyrite was formed early during early sedimentation. The second-stage pyrite is coarse-grained, euhedral and granular, 2–5 mm in size, with crystals dominated by combinations of pentagonal-dodecahedra and pentagonal-dodecahedron-cubic forms. Pyrite formed in this stage is presented as massive, disseminated, and banded aggregates and is distributed mainly within the country rocks adjacent to the ore bodies. The third-stage pyrite is medium to coarse-grained and dominated by pentagonal dodecahedra. Late-stage pyrite is presented as fine-grained cubes, 0.01–0.8 mm in size, and local pentagonal-dodecahedra, with most within dolomite in the hanging wall of the ore bodies or in fault zones near the ore bodies. Pyrite is occasionally presented in micro-veinlets and networks along fissures in galena and sphalerite (Fig. 4g). Away from the ore bodies, pyrite becomes more abundant.

Dolomite is present as coarse-grained crystals, 0.1–2 mm in grain size, and exhibits euhedral-subhedral granular textures, with distinctive signs of carbonate recrystallization. It replaces pyrite locally and forms skeletal structure. Calcite is mainly presented as massive, banded, vein and disseminated structures (Fig. 4a, b, c).

3.4 Mineralization periods

Mineralization can be divided into three periods: sedimentary, hydrothermal and weathering processes. Minerals formed during the sedimentary periods mainly dolomite, lesser pyrite (chiefly as framboidal

pyrite) and rare sphalerite. The hydrothermal period can be subdivided into the pyrite, sphalerite-galena and sphalerite-calcite stages. In the pyrite stage the minerals association are dolomite-pyrite-sphalerite-calcite. During the sphalerite-galena stage the minerals association are sphalerite-galena-calcite-dolomite. In this stage sphalerite is brown, occurs in grape and band forms caused by rapid crystallization. Galena has inclusions of Ag-bearing minerals. The minerals of a higher idiomorphic degree, which formed in the sphalerite-calcite stage, include light yellow sphalerite, calcite, galena, pyrite and a little quartz. After the deposit formed, the sulfide was weathered as smithsonite and cerussite.

4 Samples and analytical methods

All samples were collected from various parts of representative Pb-Zn deposits in the NW Guizhou Province, China. Samples from different ore-forming stages were crushed into particles (40 to 60 meshes). Calcite was selected using binocular microscope. Calcite separates were ultrasonically washed with Milli-Q ultra-pure water. Finally calcite was ground into particles smaller than 200 meshes using an agate mortar.

The carbon and oxygen isotopic compositions were analyzed using Continuous Flow Mass Spectrometer in the State Key Laboratory of Environmental Geochemistry, Institute of Geochemistry, Chinese Academy of Sciences. Errors of the $\delta^{13}\text{C}_{\text{PDB}}$ and $\delta^{18}\text{O}_{\text{PDB}}$ are all within $\pm 0.2\%$ (2σ).

5 Results

The C and O isotopic compositions of 19 hydrothermal calcite samples range from -5.3% to -0.6% (mean -3.4%) and $+11.3\%$ to $+20.9\%$ (average of $+17.2\%$), respectively. $\delta^{13}\text{C}_{\text{PDB}}$ and $\delta^{18}\text{O}_{\text{SMOW}}$ values of 9 altered wall rock-dolostone samples range from -3.0% to $+0.9\%$ (mean -1.3%) and $+17.0\%$ to $+20.8\%$ (average of $+19.7\%$), respectively. The C and O isotopic compositions of 15 carbonate rocks samples range from -1.8% to $+3.9\%$ (average of $+0.7\%$) and $+21.0\%$ to $+26.8\%$ (mean $+22.9\%$), respectively. $\delta^{13}\text{C}_{\text{PDB}}$ and $\delta^{18}\text{O}_{\text{SMOW}}$ values of 11 sedimentary calcite samples range from $+0.6\%$ to $+2.5\%$ (average of $+1.4\%$) and $+23.4\%$ to $+26.5\%$ (mean 24.6%), respectively (Table 1).

6 Discussion

6.1 Source of CO_2

The $\delta^{13}\text{C}_{\text{PDB}}$ and $\delta^{18}\text{O}_{\text{SMOW}}$ values of hydrothermal calcite, altered dolostone and host carbonate rocks

samples change widely, except for sedimentary calcites. Compared with sedimentary calcite and carbonate rocks, the hydrothermal calcite and altered dolostone samples have lower $\delta^{13}\text{C}_{\text{PDB}}$ and $\delta^{18}\text{O}_{\text{SMOW}}$ values. In the $\delta^{13}\text{C}_{\text{PDB}}$ vs. $\delta^{18}\text{O}_{\text{SMOW}}$ diagram (Fig. 5A), the samples of sedimentary calcite and carbonate rocks fall within the field of marine carbonate, in agreement with the geological features. In contrast, the samples of altered dolostone are close to the field of marine carbonate, implying that the C and O isotopic compositions of altered dolostone are controlled by marine carbonate, with decarbonation as the main factor. $\delta^{13}\text{C}_{\text{PDB}}$ and $\delta^{18}\text{O}_{\text{SMOW}}$ values of hydrothermal calcite fall into the field between marine carbonate

and the mantle. Some researchers regarded that the CO_2 in the ore-forming fluids was derived from mixing sources of crustal carbon from the cover Devonian to Permian carbonate rocks and mantle carbon from the Permian Emeishan flood basalts (Huang Zhilong et al., 2004, 2010; Han Runsheng et al., 2007). According to the homogenization temperatures of fluid inclusions in hydrothermal calcite (between 180 and 250°C; Jin Zhongguo, 2008), we think that the sedimentary contamination or high temperature effect was not the main factor, whereas the magmatic degassing may control the formation of CO_2 in the Huize carbonate-hosted Pb-Zn deposit (Huang Zhilong et al., 2010).

Table 1 $\delta^{13}\text{C}$ and $\delta^{18}\text{O}$ of NW Guizhou Pb-Zn metallogenic district, China

Deposit	Sample No.	Object	$\delta^{13}\text{C}_{\text{PDB}}/\text{‰}$	$\delta^{18}\text{O}_{\text{PDB}}/\text{‰}$	$\delta^{18}\text{O}_{\text{SMOW}}/\text{‰}$	Source	
Tianqiao Pb-Zn deposit	TQ-10	Hydrothermal calcite	-4.6	-12.1	18.4	a, k	
	TQ-13	Hydrothermal calcite	-4.2	-11.0	19.5		
	TQ-48	Hydrothermal calcite	-4.9	-12.3	18.2		
	TQ-57	Hydrothermal calcite	-5.3	-12.0	18.6		
	TQ-70	Hydrothermal calcite	-5.1	-12.2	18.3		
	TQ-08-01	Hydrothermal calcite	-3.4	-15.5	14.9		
	TQ-08-02	Hydrothermal calcite	-4.9	-11.9	18.6		
	TQ-08-03	Hydrothermal calcite	-4.4	-13.9	16.5		
	HTQ-altered rock	Altered dolostone	-3.0	-9.9	20.7		
	HTQ-wall rock	Dolostone	-0.8	-7.6	23.1		
	5 average value	Dolostone	-1.8	-7.1	23.6		
	Tianqiao-1	Altered dolostone	-1.2	-9.9	20.8		d, e
	Tianqiao-4	Altered dolostone	-0.7	-11.0	18.6		
Tianqiao-5	Altered dolostone	-2.3	-10.0	20.6			
Tianqiao-6	Altered dolostone	-2.5	-10.2	20.4			
Shanshulin Pb-Zn deposit	SSL-6	Sedimentary calcite	2.5	-4.3	26.5	j	
	SI-9	Sedimentary calcite	2.5	-5.2	25.6	f	
	S altered rock-O	Limestone	2.4	-5.3	25.5		
	Sh-S-51	Limestone	3.9	-4.0	26.8		
Shaojiwan/Hetang/ Shuicaozi Pb-Zn deposits	SJW-16	Hydrothermal calcite	-2.8	-11.2	19.3	j	
	HT-10	Sedimentary calcite	0.9	-6.1	24.6	f	
	HT-01	Sedimentary calcite	0.6	-5.5	25.2		
	STC-5	Sedimentary calcite	1.9	-6.1	24.6		
	YCP4-7	Hydrothermal calcite	-0.6	-13.0	20.9		
Yinchangpo Pb-Zn deposit	YCP3-17	Hydrothermal calcite	-3.2	-13.0	17.5	g, h	
	YCP6	Hydrothermal calcite	-1.5	-17.4	11.3		
	YCP6-A	Hydrothermal calcite	-1.5	-13.5	16.0		
	YCP6-1	Hydrothermal calcite	-2.2	-12.0	13.0		
	YCP6-3	Hydrothermal calcite	-2.6	-19.0	17.5		
	YCP2-A (C ₁ b)	Dolostone	0.8	-9.6	21.0		
	YCP2-B (C ₁ b)	Dolostone	0.8	-9.6	21.0		
	YCP3-1K (C ₁ b)	Altered dolostone	-0.3	-9.7	17.0		
	YCP3-5K (C ₁ b)	Hydrothermal calcite	-2.3	-14.4	18.5		
	HE11 (C ₁ b)	Altered dolostone	0.9	-11.2	19.3		
	HE17 (C ₁ b)	Limestone	0.9	-9.6	21.0		
	HE01 (C ₁ b)	Limestone	-1.2	-8.0	22.6		
	HE12 (C ₁ b)	Altered limestone	-1.1	-10.5	20.1		
	HE16 (C ₁ b)	Limestone	-0.4	-8.2	22.5		
	HE18 (C ₁ b)	Limestone	-1.5	-9.2	21.3		
Qingshan Pb-Zn deposit	Qs host rock-O	Limestone	2.3	-7.7	22.91	f	
	Qs altered rock-O	Limestone	1.1	-6.6	24.1		
	QS-02	Sedimentary calcite	1.8	-6.5	24.3		
	QS-03	Sedimentary calcite	1.0	-6.0	24.7		
	HT-01	Sedimentary calcite	0.6	-5.5	24.4		
	HT-10	Sedimentary calcite	0.9	-6.1	23.8		
	Qs-02	Sedimentary calcite	1.7	-6.5	23.4		
	Qs-03	Sedimentary calcite	1.0	-6.0	23.9		
	Qs-01	Limestone	2.3	-6.6	23.3		
Qs-04	Limestone	1.1	-7.7	22.1			

Note: a. Zhou Jiayi et al., 2012; b. Mao Deming, 2000; c. Zhu Laiming et al., 1998; d. Wang Huayun, 1996; e. Wang Huayun, 1993; f. Mao Jianquan et al., 1998; g. Hu Yaoguo, 1999; h. Chen Shijie, 1986; i. Zhang Qihou et al., 1999; j. this paper; k. Zhou Jiayi et al., revision. $\delta^{18}\text{O}_{\text{SMOW}}=1.03086 \delta^{18}\text{O}_{\text{PDB}}+30.86$ (Friedman and O'Neil, 1977).

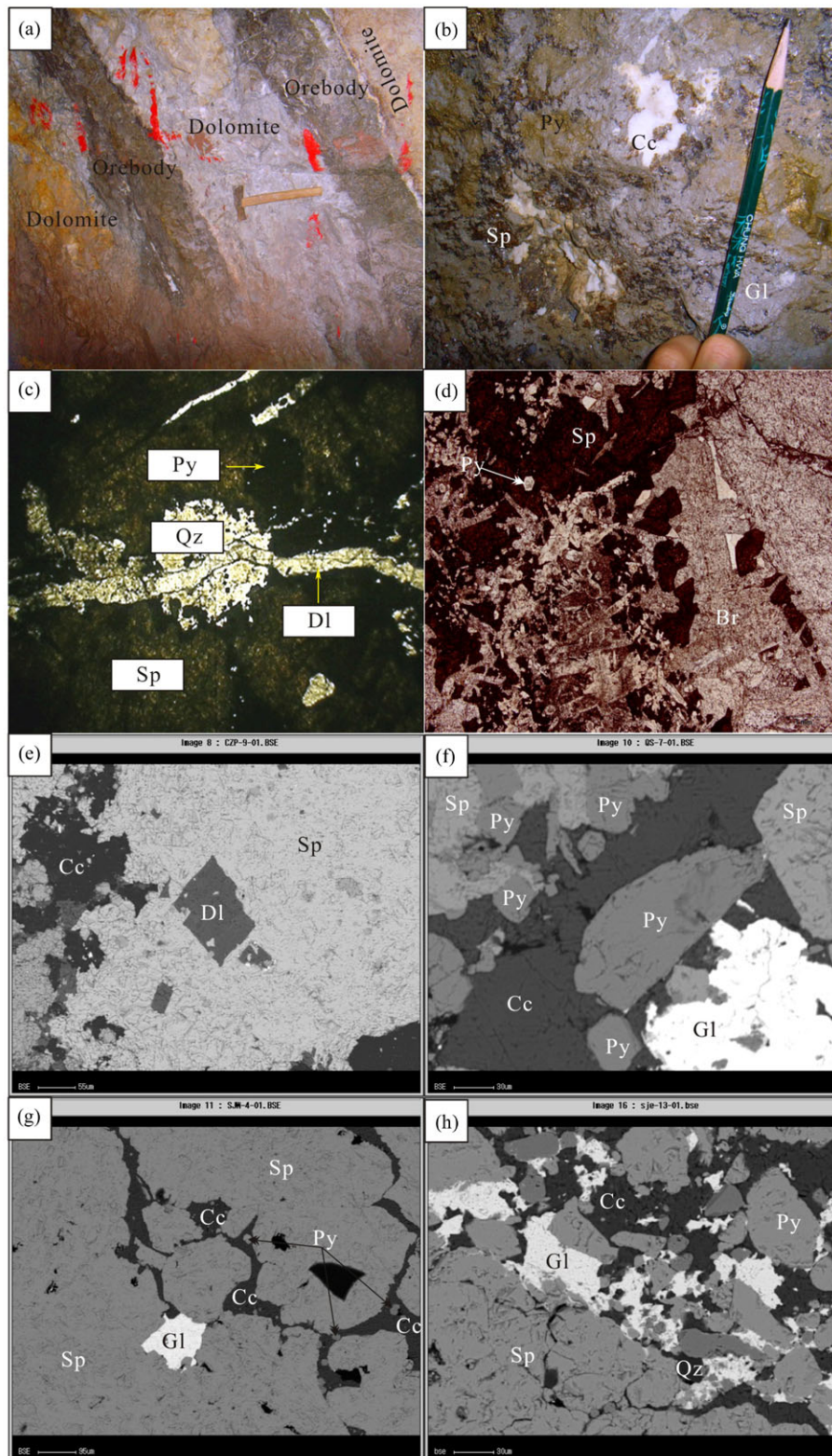


Fig. 4. Photographs of ores textures and structures from NW Guizhou Pb-Zn metallogenic province. (a) Boundaries between the ore bodies and the coarse crystalline dolomite wall rocks; (b) calcite, pyrite, sphalerite and galena symbiotic association; (c) dolomite fine vein intercalated with quartz and pyrite inclusion in sphalerite; (d) pyrite and sphalerite in barite and catalytic texture; (e) calcite and dolomite inclusion in sphalerite; (f) calcite vein intercalated with sphalerite, containing pyrite and in symbiotic association with galena; (g) galena inclusion in sphalerite, intercalated with calcite contains pyrite; (h) galena, quartz, calcite and pyrite in catalytic sphalerite. Cc. calcite; Py. pyrite; Sp. sphalerite; Gl. galena; Qz. quartz; Br. barite.

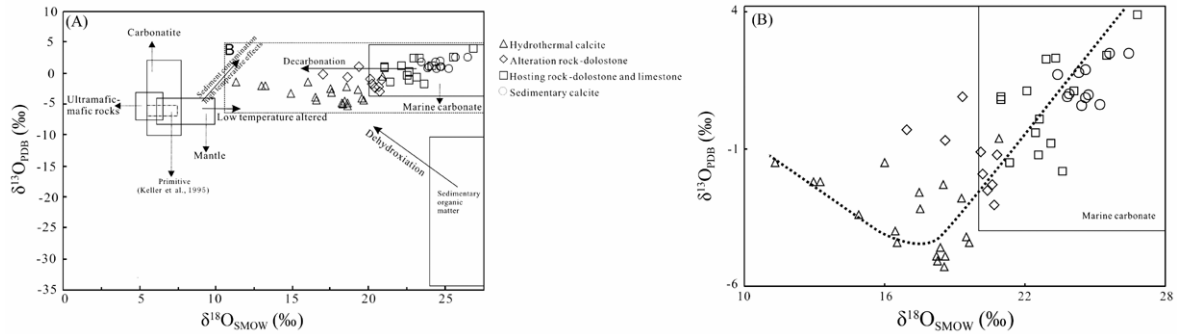


Fig. 5. Diagram of $\delta^{13}\text{C}_{\text{PDB}}$ vs. $\delta^{18}\text{O}_{\text{SMOW}}$.

However, in the $\delta^{13}\text{C}_{\text{PDB}}$ vs. $\delta^{18}\text{O}_{\text{SMOW}}$ diagram (Fig. 5B), the relationship between $\delta^{13}\text{C}_{\text{PDB}}$ and $\delta^{18}\text{O}_{\text{SMOW}}$ values of hydrothermal calcite samples is negatively correlated with a curve correlation relationship between samples. Based on the diagram of $\delta^{13}\text{C}_{\text{PDB}}$ vs. $\delta^{18}\text{O}_{\text{SMOW}}$ (Fig. 5A), marine carbonate dissolution leads to unchanged $\delta^{13}\text{C}_{\text{PDB}}$ but depletion of $\delta^{18}\text{O}_{\text{SMOW}}$. Low temperature altered of Mantle leads to unchanged $\delta^{13}\text{C}_{\text{PDB}}$ but enrichment of $\delta^{18}\text{O}_{\text{SMOW}}$. Therefore, the two models couldn't explain the curve correlation between $\delta^{13}\text{C}_{\text{PDB}}$ and $\delta^{18}\text{O}_{\text{SMOW}}$. Sedimentary contamination or high temperature effect of Mantle result in higher $\delta^{13}\text{C}_{\text{PDB}}$ and $\delta^{18}\text{O}_{\text{SMOW}}$ values, and it isn't the factor based on the homogenization temperatures of fluid inclusions (between 180 and 250°C; Jin Zhongguo, 2008). Dehydroxylation of sedimentary organic matter results in higher $\delta^{13}\text{C}_{\text{PDB}}$ and lower $\delta^{18}\text{O}_{\text{SMOW}}$ values, but those C and O isotopic compositions in the studied samples deviate from the field that of sedimentary organic matter, raising the conclusion that the dehydroxylation of sedimentary organic matter isn't the main factor too.

Association with other evidences (such as Sr isotopic compositions), we considered that the forming mechanism of CO_2 in the ore-forming fluids involves the concurrent event of marine carbonate dissolution (Zhou Jiayi et al., 2012), dehydroxylation of sedimentary organic matter (this paper) and magmatic degassing (Huang Zhilong et al., 2010). Of course, CO_2 in ore-forming fluids was derived mainly from the carbonate rocks, consistent with the carbonate-hosted Pb-Zn deposits around world (Richardson et al., 1988; Spangenberg et al., 1996; Large et al., 2001; Wilkinson et al., 2005; Marshall et al., 2006). The sedimentary organic matter was carried by ore-forming fluids from sand-shale of the Lower Permian Liangshan Formation, the process of which will be explained in terms of the ore genesis model (Fig. 6).

6.2 Sources of water

H and O isotopic compositions from this province are limited. The only reported δD values of cal-

cite inclusions from the Shanshulin deposit was collected, with ranging from -55‰ to -46‰ (Mao Jianquan et al., 1998). Based on the $\delta^{18}\text{O}$ values of calcite, the $\delta^{18}\text{O}_{\text{H}_2\text{O}}$ values are converted ($1000 \ln a_{\text{calcite-H}_2\text{O}} = 4.01 \times 10^6/T^2 - 4.66 \times 10^3/T + 1.71$, $T=200^\circ\text{C}$; Zheng Yongfei and Chen Jiangfeng, 2000). The obtained $\delta^{18}\text{O}_{\text{H}_2\text{O}}$ values of water in the ore-forming fluids are range from +1.8‰ to +17.0‰, with a mean value of +10.5‰, and fall between metamorphic water and atmospheric water in the δD vs. $\delta^{18}\text{O}_{\text{H}_2\text{O}}$ diagram, indicating that the water is the mixture of metamorphic and atmospheric waters. δD and $\delta^{18}\text{O}_{\text{H}_2\text{O}}$ isotopic compositions of calcites from the Huize carbonate-hosted Pb-Zn deposit range from -75‰ to -55.8‰ and -8.04‰ to +6.44‰, respectively, which are explained to be of mixing origin from magmatic and metamorphic waters (Huang Zhilong et al., 2004; Han Runsheng et al., 2007). Based on the water-rock reaction calculation (Huang Zhilong et al., 2004; Jin Zhongguo, 2008), it is believed that the ore-forming fluid is the mixture of metamorphic, magmatic and atmospheric waters.

6.3 Genesis of the deposits

There are three major types of Pb-Zn deposit, SEDEX-type, VHMS (VMS)-type and MVT-type. Agreed by many scientists, the genetic type of Pb-Zn deposits in this province belongs neither to SEDEX nor to VHMS (VMS) (Tu Guangchi, 1984; Liu Hechang and Lin Wenda, 1999; Hu Yaoguo, 1999; Mao Deming, 2000; Liu Youping, 2002; Huang Zhilong et al., 2004; Han Runsheng et al., 2007; Li Wenbo et al., 2007; Jin Zhongguo, 2008; Zhou Jiayi et al., 2009, 2010a, b). However, it is also different from typical MVT deposits. The obviously differences include tectonic setting, ore grade and relationship with basalts (Liu Hechang and Lin Wenda, 1999; Hu Yaoguo, 1999; Mao Deming, 2000; Liu Youping, 2002; Huang Zhilong et al., 2004; Han Runsheng et al., 2007; Li Wenbo et al., 2007; Jin Zhongguo, 2008).

Detailed difference as follow: (1) high grade of these deposits in this province ($\text{Zn}+\text{Pb} \geq 20$ wt%,

mostly higher than 25 wt%) (Jin Zhongguo, 2008; Zhou Jiayi et al., 2010b); (2) containing multiple metals, including Ag, Ge, In, Ga, Cd, and Tl (Zhou Jiayi et al., 2010b); (3) simple and limited wall-rock alteration, e.g. dolomitization (Jin Zhongguo, 2008); (4) ore distribution being controlled by both thrust-nappe tectonic and lithology (Han Runsheng et al., 2007); (5) evaporite layers in the host carbonate rocks of the Devonian, Carboniferous and basement rocks, which are the source of sulfur; (6) single gangue minerals, calcite and dolomite; and (7) the genetic relationship between the Permian flood basalts and Pb-Zn mineralization in the region (Huang Zhilong et al., 2004; Han Runsheng et al., 2007).

These deposits were situated in three later Paleozoic thrust fault belts (Fig. 2), which formed later than hosting rocks. Therefore, the geological and tectonic features indicate that the deposits were epigenetic (e.g. Jin Zhongguo, 2008; Zhou Jiayi et al., 2009).

C-O-S and Pb-Sr isotopic compositions show that the sulfur in the ore-forming fluids should be derived from marine sulfates by thermal chemical sulfate reduction (Zhou Jiayi et al., 2010a, b). CO₂ was originated from carbonate rocks sedimentary organic matter and magmatic degassing (Zhou Jiayi et al., 2012; this paper). Lead has crust-derived features and is formed by mixing of Sinian to Permian carbonate rocks, basement rocks and the Emeishan flood basalts (Jin Zhongguo, 2008; Zhou Jiayi et al., 2010a). Ore-forming fluids might be derived from or flow through basement rocks constrains from Sr isotope (Hu Yaoguo, 1999). Compared with altered wall rocks, hosting carbonate rocks, basement rocks and Emeishan flood basalts (Zhou Jiayi et al., 2011, 2012), REE in calcite and sulfides were sourced mainly from the hosting carbonate rocks.

All the discussion above favor that the genetic type may be explained by epigenetic multiple source, whereas the carbonate-hosted type is genetically associated with the hosting carbonate rocks, Sinian to Permian sedimentary rocks, Precambrian basement rocks and Permian Emeishan flood basalts.

6.4 A possible model for these deposits

The Paleozoic basement rocks are enriched in Pb, Zn, and other ore-forming metals, which could be the ultimate source of metals for the ore forming fluids (Huang Zhilong et al., 2004). The Paleozoic carbonate rocks from the Early Devonian Danlin Formation to the Early Permian Qixia-Maokou Formation are mostly filled with gypsum-salt beds and also contain certain amounts of Pb, Zn, and other ore-forming elements (Zhou Jiayi et al., 2010b).

Extensive fluid migration and circulation resulted

in reduction of sulfur to thiosulfate and hydrosulphuric acid in the gypsum-salt bed, and the thiosulfate and hydrosulphuric acid, leaching ore-forming elements in the basement and all strata, form ore-forming fluids. Driven by tectonic and thermal dynamics, the ore-forming fluids migrated upwards along regional faults including the Yadu-Mangdong and Shuicheng-Weining faults and were precipitated to form the Pb-Zn ore bodies along fracture zones and interformational faulted zone structures (Fig. 6).

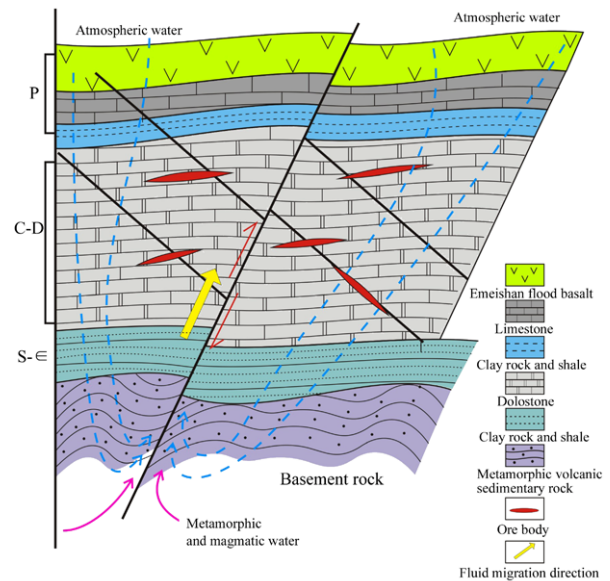


Fig. 6. Ore genetic model for the deposits in the NW Guizhou Pb-Zn metallogenic province.

7 Conclusions

Geology and C-O isotopic compositions indicate that the Pb-Zn deposits in the NW Guizhou Province were formed by fluids mixing, which were derived from hosting carbonate rocks, Sinian to Permian sedimentary rocks, Precambrian basement rocks (Kunyang and Huili groups) and Permian Emeishan flood basalts. The ore genetic type is epigenetic with multiple sources of ore forming fluids and metals, and is carbonate-hosted type hydrothermal Pb-Zn deposits.

Acknowledgements This research project was financially supported jointly by the National Natural Science Foundation of China (Grant Nos. 41102055 and 41102053) and the National Basic Research Program of China (Grant No. 2007CB411402). The authors wish to thank Professor Qi Liang (Institute of Geochemistry, CAS) and Professor Xu Cheng (Peking University) for their insightful suggestions and help in improving the quality of the manuscript.

References

- Chen Shijie (1984) A discussion on the sedimentary origin of Pb-Zn deposits in western Guizhou and northeastern Yunnan [J]. *Guizhou Geology*. **8**, 35–39 (in Chinese with English abstract).
- Chen Shijie (1986) A discussion on the origin of Pb-Zn deposits in western Guizhou and northeastern Yunnan [J]. *Guizhou Geology*. **3**, 211–222 (in Chinese with English abstract).
- Gu Shangyi (2006) Characteristics of REE composition within Pb-Zn deposits in northwestern Guizhou: In addition to a discussion of relationship between Pb-Zn deposits and Emeishan basalts in northwestern Guizhou [J]. *Guizhou Geology*. **23**, 274–277 (in Chinese with English abstract).
- Gu Shangyi (2007) Study on the sulfur isotope compositions of lead-zinc deposits in northwestern Guizhou Province [J]. *Journal of Guizhou University of Technology*. **36**, 8–13 (in Chinese with English abstract).
- Han Runsheng, Chen Jin, Li Yuan, Gao Derong, and Ma Deyun (2001) Discovery of concealed No. 8 orebody at Qilinchang lead-zinc deposit in Huize Mine, Yunnan [J]. *Geology Geochemistry*. **29**, 191–195 (in Chinese with English abstract).
- Han Runsheng, Liu Congqiang, Huang Zhilong, Chen Jin, Ma Deyun, Li Lei, and Ma Gengsheng (2007) Geological features and origin of the Huize carbonate-hosted Zn-Pb-(Ag) District, Yunnan, South China [J]. *Ore Geology Reviews*. **31**, 360–383.
- Hu Yaoguo (1999) *Occurrence of Silver, Sources of Mineralized Substances and Ore-forming Mechanism of Yinchangpo Silver-poly-metallic Deposit, Guizhou Province, China* [D]. pp.67. Doctor's Degree Dissertation, Institute of Geochemistry, CAS, Guiyang (in Chinese with English abstract).
- Huang Zhilong, Chen Jin, Han Runsheng, Li Wenbo, Liu Congqiang, Zhang Zhengliang, Ma Deyun, Gao Derong, and Yang Hailin (2004) *Geochemistry and Ore-formation of the Huize Giant Lead-zinc Deposit, Yunnan Province, China: Discussion on the Relationship Between Emeishan Flood Basalts and Lead-Zinc Mineralization* [M]. pp.1–230. Geological Publishing House, Beijing (in Chinese).
- Irving Friedman and James R.O'Neil (1977) Compilation of stable isotope fractionation factors of geochemical interest. In *Data of Geochemistry* (sixth edition), U.S. Geological Survey Professional Paper (ed. Michael F.) [M], pp.1–9. 440-KK.
- Jin Zhongguo (2008) *The Ore-control Factors, Ore-forming Regularity and Forecasting of Pb-Zn Deposit, in Northwestern Guizhou Province* [M]. pp.1–105. Engine Industry Press, Beijing (in Chinese).
- Leach D.L. and Sangster D.F. (1993) Mississippi valley-type lead-zinc deposit. In *Mineral Deposit Modeling* (eds. Kirkham R.V., Sinclair W.D., Thorpe R.I., and Duke J.M.) [M]. Geological Association of Canada, Spe. Papers, **40**, 289–314.
- Li Wenbo, Huang Zhilong, and Qi Liang (2007) REE geochemistry of sulfides from the Huize Zn-Pb ore field, Yunnan Province: Implication for the sources of ore-forming metals [J]. *Acta Geologica Sinica* (English edition). **81**, 442–449.
- Liu Hechang and Lin Wenda (1999) *Study on the Law of Pb-Zn-Ag Ore Deposits in Northeast Yunnan, China* [M]. pp.1–389. Yunnan University Press, Kunming (in Chinese).
- Liu Hechang (1996) Zn-Pb-(Ag) source beds (rocks) in the Yunnan, Sichuan and Guizhou metallogenic provinces [J]. *Journal of Geology and Exploration*. **32**, 12–18 (in Chinese with English abstract).
- Liu Youping (2002) Preliminary study on the metallogenic regulation and the prospecting model for the Pb-Zn deposits in the areas of North-west Guizhou [J]. *Guizhou Geology*. **19**, 169–174 (in Chinese with English abstract).
- Mao Deming (2000) Oxygen and carbon isotope in Guizhou Tianqiao Pb-Zn deposit [J]. *Journal of Guizhou University of Technology*. **29**, 8–11 (in Chinese with English abstract).
- Mao Deming (2001) REE geochemistry of Pb-Zn deposits in northwestern Guizhou and its significance [J]. *Guizhou Geology*. **18**, 12–17 (in Chinese with English abstract).
- Mao Jianquan, Zhang Qihou, and Gu Shangyi (1998) *Tectonic Evolution and Pb-Zn Mineralization of Shuicheng Fault Subsidence* [M]. pp.104–129. Guizhou Science and Technology Press, Guiyang (in Chinese).
- Marshall L., Oliver N., and Davidson (2006) Carbon and oxygen isotope constraints on fluid sources and fluid—Wall rock interaction in regional alteration and iron-oxide—Copper-gold mineralization, eastern Mt. Isa Block, Australia [J]. *Mineralium Deposita*. **41**, 429–452.
- Qian Jianping (2001) Tectonic-dynamic mineralization in Wein-ing-Shuicheng Pb-Zn ore belt, northwestern Guizhou [J]. *Geology-Geochemistry*. **29**, 134–139 (in Chinese with English abstract).
- Richardson S.M., and Hanse K.S. (1988) Stable isotopes in sulfate evaporates from southeastern Iowa: A clue to the history of groundwater [J]. *Eos, Transactions, American Geophysical Union*. **69**, 1515.
- Sangster D.F. (1996) Mississippi valley-type lead-zinc. In *Geology of Canadian Mineral Deposit Type* (eds. Eckstand O.R., Sinclair W.D., and Thorpe R.I.) [M]. **8**, 253–261.
- Tang Shengning (1984) Deposit model and characteristic of strata-bound Pb-Zn deposits in the northwestern Guizhou and northeastern of Yunnan Province [J]. *Journal of Geology and Exploration*. **20**, 1–8 (in Chinese).
- Tu Guangchi (1984) *The Geochemistry of Strata Bound Deposit, China* [M]. pp.13–54. Geology Press, Beijing (in Chinese).
- Wang Huayun (1993) Geochemistry of Pb-Zn mineralization in Guizhou [J]. *Guizhou Geology*. **10**, 272–290 (in Chinese with English abstract).
- Wang Huayun (1996) A genetic model for mineralization of the zinc-lead belts in eastern Guizhou [J]. *Guizhou Geology*. **13**, 7–23 (in Chinese with English abstract).
- Wang Wei and Zhou Meifu (2012) Sedimentary records of the Yangtze Block (South China) and their correlation with equivalent Neoproterozoic sequences on adjacent continents [J]. *Sedimentary Geology*. **265–266**, 126–142.
- Wilkinson J.J., Eyre S.L., and Boyce A.J. (2005) Ore-forming processes in Irish-type carbonate-hosted Zn-Pb deposits: Evidence from mineralogy, chemistry, and isotopic composition of sulfides at the Lisheen Mine [J]. *Econ. Geol.* **100**, 63–86.
- Xie Jiarong (1963) *Introduction of the China's Ore Deposits* [M]. pp.1–305. Science Press, Beijing (in Chinese).
- Zhang Qihou, Gu Shangyi, and Mao Jianquan (1999) Geochemical study on qingshan Pb-Zn deposit in Shuicheng, Guizhou Province [J]. *Geology-Geochemistry*. **27**, 15–20 (in Chinese with English abstract).
- Zheng Chuanglun (1992) Study on ore-controlling structures of Pb-Zn ore region in northwestern Guizhou Province [J]. *Mineral Resources and Geology*. **6**, 193–200 (in Chinese with English abstract).
- Zheng Chuanglun (1994) An approach on the source of ore-forming metals of Pb-Zn deposits in northwestern Guizhou Province [J]. *Journal of*

- Guilin College of Geology*, **14**, 113–124 (in Chinese with English abstract).
- Zheng Yongfei and Chen Jiangfeng (2000) *Geochemistry of Stable Isotope* [M]. pp.40–41. Science Press, Beijing (in Chinese).
- Zhou Jiayi, Huang Zhilong, Zhou Guofu, Li Xiaobiao, Ding Wei, and Bao Guangping (2011) Trace elements and rare earth elements of sulfide minerals in the Tianqiao Pb–Zn ore deposit, Guizhou Province, China [J]. *Acta Geologica Sinica* (English edition). **85**, 189–199.
- Zhou Jiayi, Huang Zhilong, Zhou Guofu, Li Xiaobiao, Ding Wei, and Bao Guangping (2010a) Sulfur isotopic compositions of the Tianqiao Pb–Zn ore deposit, Guizhou Province, China: Implications for the source of sulfur in the ore-forming fluids [J]. *Chinese Journal of Geochemistry*. **29**, 301–306.
- Zhou Jiayi, Huang Zhilong, Zhou Guofu, Jin Zhongguo, Li Xiaobiao, Ding Wei, and Gu Jing (2010b) Sources of the ore metals of the Tianqiao Pb–Zn deposit in northwestern Guizhou Province: Constraints from S, Pb isotope and REE Geochemistry [J]. *Geological Review*. **56**, 513–524 (in Chinese with English abstract).
- Zhou Jiayi, Huang Zhilong, Zhou Guofu, Li Xiaobiao, Ding Wei, and Gu Jing (2009) The occurrence state and regularity of dispersed elements in Tianqiao Pb–Zn ore deposit, Guizhou Province, China [J]. *Acta Mineralogica Sinica*. **29**, 471–480 (in Chinese with English abstract).
- Zhou Jiayi, Huang Zhilong, Zhou Guofu, and Zeng Qiaosong (2012) C, O isotope and REE geochemistry of hydrothermal calcite from the Tianqiao Pb–Zn ore deposit in NW Guizhou Province, China [J]. *Geotectonica et Metallogenia*. **36**, 93–101 (in Chinese with English abstract).
- Zhou Jiayi, Huang Zhilong, Zhou Meifu, Li Xiaobiao, and Jin Zhongguo. Constraints of C–O–S–Pb isotopic compositions and Rb–Sr isotopic age on the origin of the Tianqiao carbonate-hosted Pb–Zn deposit, SW China [J]. *Ore Geology Reviews* (revision).
- Zhou Meifu, Malpas J., Song Xieyang, Robinson P.T., Sun Ming, Kennedy A.K., Leshner C.M., and Keays R.R. (2002) A temporal link between the Emeishan large igneous province (SW China) and the end–Guadalupian mass extinction [J]. *EPSL*. **196**, 113–122.
- Zhu Laiming, Luan Shiwei, Yuan Haihua, and Qi Huawen (1998) “Double source” sedimentary—Transformation metallogenic model of the Disu Pb–Zn deposit [J]. *Mineral Deposits*, **17**, 82–90 (in Chinese with English abstract).